ELSEVIER

Synthetic Metals 125 (2002) 107–116

SYNTHETIC METALS

www.elsevier.com/locate/synmet

Electronic structure of π-conjugated oligomers and polymers: a quantum–chemical approach to transport properties

J.L. Brédas[a,b,*], D. Beljonne[a,b], J. Cornil[a,b], J.Ph. Calbert[a,b], Z. Shuai[b], R. Silbey[c]

[a]*Department of Chemistry, The University of Arizona, Tucson, AZ 85721-0041, USA*

[b]*Service de Chimie des Matériaux Nouveaux, Centre de Recherche en Electronique et Photonique Moléculaires, Université de Mons-Hainaut, Place du Parc 20, B-7000 Mons, Belgium*

[c]*Department of Chemistry and Center for Materials Science and Engineering, Massachusetts Institute of Technology, Cambridge, MA 02139-4307, USA*

Abstract

Nearly 25 years after the discovery that an organic conjugated polymer can be ''doped'' (that is, in chemical terminology, oxidized or reduced) to metallic-like electrical conductivity, the field of π-conjugated oligomers and polymers has enjoyed a tremendous development, most remarkably underlined by the 2000 Nobel Prize in Chemistry awarded to Alan Heeger, Alan MacDiarmid, and Hideki Shirakawa. Since, in this specific class of polymers, small variations in chemical structure play an essential role and the properties of interest directly depend on the electronic structure, quantum–chemical approaches, that take the chemical nature fully into account, have provided a most valuable input to the field. The results have helped to forge a fundamental understanding of the electronic and optical properties of π-conjugated materials and in guiding the experimental efforts toward novel compounds with enhanced characteristics. It is our main purpose in this contribution to illustrate the impact of quantum–chemical methods, more specifically in relation to transport processes. We do not dwell at all on the theoretical methodologies that have been designed, but rather on the concepts. We first recall the basic electronic-structure aspects of π-conjugated systems, that make their chemistry and physics so rich and fascinating. We then discuss the key role of interchain interactions and their impact on transport.

Keywords: Oligomers; Polymers; Conductivity; Transport; Interchain interactions

1. Basic aspects of the electronic structure of π-conjugated oligomers and polymers

The determination of the electronic structure of π-conjugated systems might at first glance be considered as an easy task. Indeed, every chemist remembers that the first and most simple quantum–chemical method he/she has been introduced to, the one-electron Hückel technique, is mainly designed for conjugated molecules. However, the properties that are nowadays dealt with require a proper description of electronic excited states and interchain interactions, for which the role of many-body effects is significant. In this context, the theoretical treatment of π-conjugated systems often becomes elaborate because of the need: (i) to incorporate electron correlation effects; and (ii) to take account of the strong connection between, and mutual influence of, the electronic and geometric structures.

That electron correlation effects are important can be seen from an analysis of the ordering of the lowest singlet excited states in polyenes and polyacetylene [1]. We take the simple example of octatetraene, Fig. 1. A one-electron (e.g. Hückel or Hartree–Fock) treatment produces eight π-MOs whose symmetries alternate between ''gerade'' (g) and ''ungerade'' (u) and energies increase with the number of nodes in the wavefunction [2]. The eight π-electrons distribute among the eight π-MOs, each of their possible repartitions corresponding to a so-called electronic configuration (whose wavefunction can be cast in the form of a single Slater determinant). At the one-electron level, the lowest energetic configuration corresponds to the situation where the π-electrons occupy 2 by 2 the four lowest π-MOs and defines the singlet ground state S_0 (of A_g symmetry); the lowest (one-photon allowed) excited state (of B_u symmetry) is described by promotion of a single electron from highest occupied molecular orbital (HOMO) to lowest unoccupied molecular orbital (LUMO); any (one-photon forbidden) A_g excited state lies higher in energy because, for instance, promotion of a single electron from HOMO to LUMO + 1

* Corresponding author. Tel.: +1-250-626-6561; fax: +1-520-621-8407.
E-mail address: jlbredas@u.arizona.edu (J.L. Brédas).

0379-6779/01/$ – see front matter
PII: S0379-6779(01)00517-3

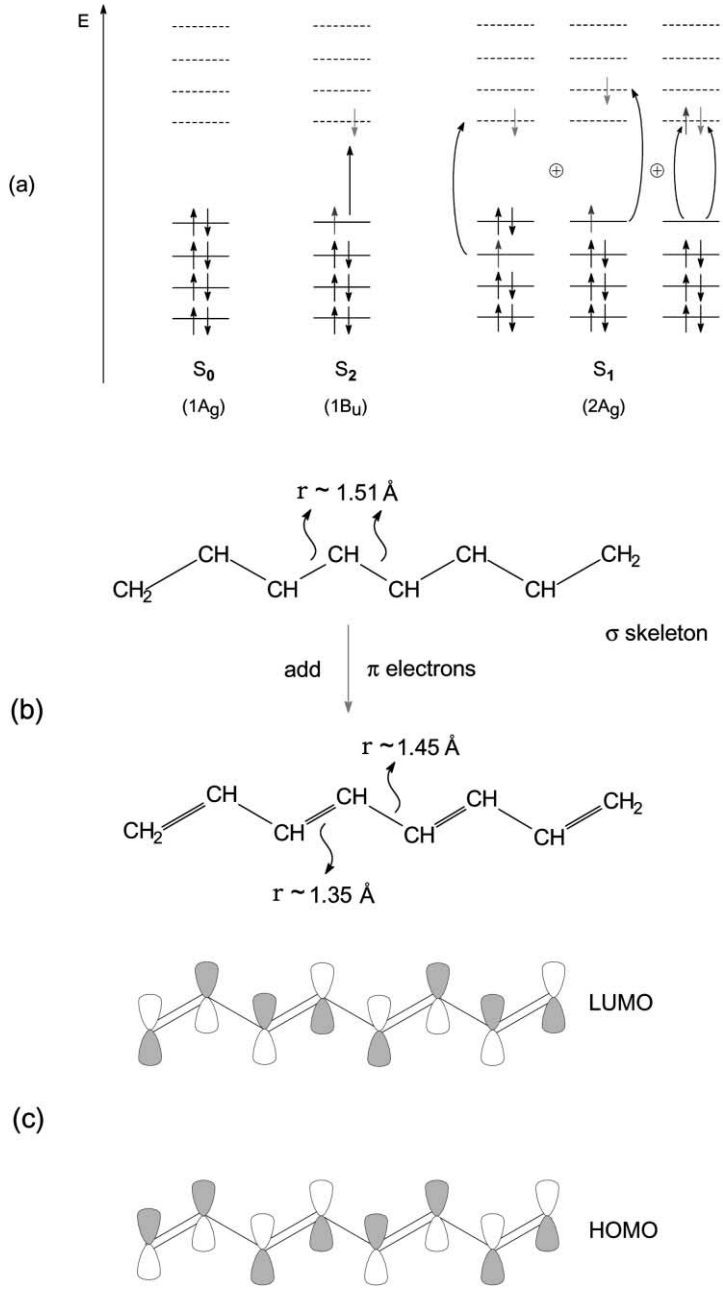

Fig. 1. Schematic illustration, in the case of octatetraene CH_2=CH–CH=CH–CH=CH–CH=CH_2, of: (a) the main electronic configurations contributing to the ground state S_0 and the lowest singlet excited state S_1 and S_2; (b) the ''dimerization'' of the geometric structure due to the uneven distribution of the π-electrons over the bonds; and (c) the bonding–antibonding pattern of the HOMO and LUMO levels.

or HOMO − 1 to LUMO or promotion of two electrons from HOMO to LUMO nominally costs a larger energy.

However, an entirely different picture emerges when electron correlation is switched on. Various methods have been developed to take account of electron correlation [3]; for instance, in the configuration interaction (CI) approach, each state is cast into a linear combination of electronic configurations (the corresponding wavefunctions are then described by a linear combination of Slater determinants). In polyenes, it so happens that the singly excited HOMO to LUMO + 1 and HOMO − 1 to LUMO and doubly excited HOMO to LUMO configurations strongly mix and result in the $2A_g$ state being located below the $1B_u$ state; in other words, in polyenes (at least those longer than butadiene), the lowest excited singlet state, S_1, is one-photon forbidden with respect to the ground state. The consequence is that polyenes and polyacetylene do not luminesce. According to Kasha's rule, luminescence takes place from the lowest excited state [4,5]; in order to observe strong fluorescence, a large one-photon coupling between S_0 and S_1 is required [6].

A major specificity of conjugated compounds is the interconnection between electronic structure and geometric

structure that has been beautifully exemplified in the field of conducting polymers with the emergence of the concepts of solitons, polarons, and bipolarons [7–9]. Consider again octatetraene, Fig. 1, and suppose that, in a first step, only the σ backbone is taken into account. The geometry is then such that all carbon–carbon bond lengths are roughly the same and equal to ca. 1.51 Å (the typical single bond length between two sp^2 carbons). When the π-electrons are thrown in, the main point is that they distribute unevenly over the bonds and in such a way that there is alternating larger and smaller π-bond densities when starting from one end of the molecule, resulting in alternating double-like carbon–carbon bonds (ca. 1.35 Å long) and single-like bonds (ca. 1.45 Å long). A notable feature is that this geometry is reflected in the bonding–antibonding pattern of the HOMO wavefunction while the LUMO wavefunction displays exactly the opposite bonding–antibonding pattern, see Fig. 1. It is then easily understood that, in the $1B_u$ excited state (that mainly involves promotion of one electron from HOMO to LUMO), the π-bond densities are strongly modified; as a consequence, the equilibrium geometry in the $1B_u$ state is markedly different from that in the ground state. All other π-excited states also have equilibrium geometries determined by their π-bond density distributions. Note that as the molecules get longer, the geometry relaxation no longer affects the whole chain, but becomes localized (in the $1B_u$ state, the optimal relaxation extends over some 20–25 Å [10]).

Another manifestation of the twinning between the geometric and electronic structures is the dependence of the ordering of the lowest singlet excited states on the effective degree of bond-length alternation, δ, along the backbone [11]. As δ increases, e.g. when switching from a purely polyenic backbone as in polyacetylene, to a mixed aromatic-polyenic backbone, as in poly(*p*-phenylene vinylene) (PPV), the $2A_g$ state gets destabilized versus the $1B_u$ state, up to the point that $1B_u$ becomes the lowest singlet S_1 state [11]. As a result, PPV and its derivatives strongly luminesce and are incorporated as emissive layers in polymer-based light-emitting diodes [12,13].

2. Transport properties

2.1. Highly organized molecular materials

The transport properties in organic media have been often described theoretically in the framework of macroscopic phenomenological models where the main parameters are usually fitted from experimental data [4,5,14–17]. These models address in a detailed way the effect of temperature and the dual role of lattice vibrations in confining the charged species over individual units through geometry relaxation phenomena and in assisting the drift of the charges across the material. Quantum–chemical calculations can prove complementary to these phenomenological models by providing quantitative estimates of important parameters governing the transport properties, as has been illustrated in a recent work on discotic liquid crystals [18]. The goal of the calculations is then: (i) to characterize the nature of the HOMO and LUMO one-electron levels of the isolated oligomer/polymer chains; and (ii) to determine the splitting of these levels due to interchain interactions. This splitting leads to the formation of valence and conduction bands at the scale of large molecular clusters/crystals.

At very low temperature, the transport mechanisms in well-ordered materials can be described in terms of band-like motion; this is the case, for instance, in the single crystals of the α-sexithienyl (6T), α-quaterthienyl (4T), and pentacene oligomers, as shown by the results of recent mobility measurements [19–21]. In this regime, the current flows under the form of either polarons delocalized over several chains or free carriers. The total valence and conduction bandwidths built from the interaction of the HOMO and LUMO levels are then the key parameters governing the hole and electron mobilities. In the framework of tight-binding models (the underlying theory is developed for instance in [22]), the total valence and conduction bandwidth of an infinite one-dimensional stack is equal to four times the corresponding interchain transfer integral. As temperature increases, low-energy vibrational modes, such as librations, start impeding the mobility of the charge carriers.

At room temperature, the charge carriers are expected to be localized over a single unit (due to the strong electron–phonon coupling underlined above); this leads to geometry relaxation under the form of localized positive or negative polarons. The transport mechanism can then be described in terms of sequential jumps of the relaxed charges between adjacent chains (also referred to as thermally activated polaronic hopping processes). The interchain transfer integral is, thus, also here a critical parameter since the rate (k_{et}) for charge hopping in the high temperature range can be expressed from Marcus theory in a simplified way as [23–27]

$$k_{et} = \left(\frac{4\pi^2}{h}\right) t^2 (4\pi\lambda RT)^{-0.5} \exp\left(\frac{-\lambda}{4RT}\right)$$

where λ is the internal reorganization term proportional to the geometric relaxation energy of the charged species over the individual units. This relation illustrates that the rate of transfer of a localized polaron from a singly charged molecule to a neutral molecule is considerably slowed down by the fact that then the two molecules have initially different geometries. As a result, vibrations can come into play to favor reaching a transition state where the two molecules have the same geometry.

Globally, the dual role of the vibrations is reflected by the fact that the electron and hole mobilities are reduced by up to five-orders of magnitude when going from the low to the high temperature range; this evolution has been recently observed with remarkable detail in the case of pentacene

and other herringbone-stacked molecular single crystals [19,28,29]. Note that the amplitude of the electron–phonon coupling (and thus the relaxation energy) typically decreases as the inverse number of atoms involved in the π-conjugated backbone and, hence, quickly saturates with the size of the oligomer [30].

These considerations illustrate that a relevant issue to be addressed by quantum–chemical studies is to examine the variation in the amplitude of the interchain transfer integrals as a function of the nature and relative positions of the interacting units. The molecular structural data (usually extracted from crystalline structures) are used to build clusters in a specific way, in order to investigate the influence of the relative positions of the molecules/chains on the electronic splittings. The electronic structure of the clusters is computed with the help of the so-called spectroscopic parameterization of the semiempirical Intermediate Neglect of Differential Overlap (INDO(s)) Hamiltonian developed by Zerner and co-workers [31,32] (the electron repulsion terms being expressed by means of the Mataga–Nishimoto potential [33]). The reliability of the INDO method to describe intermolecular interactions in molecular assemblies has been recognized in earlier theoretical studies ([34] and references therein).

We have compared the electronic structure in the single crystals of pentacene, α-sexithienyl (6T), and bisdithienothiophene (BDT), see Fig. 2; all these materials are attractive for use in field-effect transistors. The single crystal of pentacene grows in the triclinic space group $P_{1/2}$,[1] and is characterized by a herringbone packing of the molecules within stacked layers; such a molecular arrangement would, at first sight, be expected to lead to rather weak overlap between the electronic wavefunctions of the individual molecules. A similar chain packing is observed in the monoclinic single crystals of the widely studied 6T in both the low- and high-temperature (LT and HT) phases [35,36] (note that the terminology used to label these two phases refer to the fact that LT is crystallized by vapor deposition at a temperature source lower than that used for HT; both phases are actually stable over the whole temperature range typically probed by mobility measurements). In contrast, the crystal structure of BDT [37] displays a strong orbital overlap for molecules stacked along the *b*-axis (Fig. 2); this is expected to impact strongly the transport properties and bring significant differences with respect to 6T and pentacene. Note that the two inequivalent molecules within the layers of the pentacene single crystal (labeled 1 and 2 in Fig. 2) have slightly different geometries; this feature, which is not found in the 6T crystals, cannot be attributed to statistical fluctuations during the X-ray data collection; as a result, there exists a difference in the energy of the HOMO and LUMO levels of the inequivalent molecules, which is calculated to be 61 and 70 meV, respectively [38].

[1] The crystal structure has been obtained by T. Siegrist (Lünd University) and provided to us by J.H. Schön and B. Batlogg.

In the three crystalline structures under investigation, the interchain transfer integrals between molecules located in adjacent layers (i.e. for example along the *a*-axis in 6T) are negligible. Thus, charge transport takes place predominantly within the layers, as confirmed by experimental data [20,21,39]. In the pentacene and 6T single crystals, there are several directions within the layers giving rise to significant electronic splittings, namely along the axis connecting the closest equivalent molecules (i.e. the *c*-axis in the 6T crystal, see Fig. 2) and the diagonal axes *d* linking inequivalent molecules.

We first examine one-dimensional clusters formed by 6T molecules stacked along either the *a*- or *d*-axis and built from the LT crystalline phase. Fig. 3 shows the evolution of the bandwidth formed by the HOMO and LUMO levels upon interaction, as a function of $\cos(\pi/N+1)$, where N is the number of chains in the clusters. These results show that: (i) the electronic splittings saturate rapidly with cluster size; thus, band-structure calculations using periodic conditions are not necessarily required to get an insight into the transport properties of the crystal; and (ii) the splitting of the LUMO level is systematically *larger* than that calculated for the HOMO level. Thus, whatever the charge transport mechanism involved (band versus hopping regime), electrons are expected to be more mobile than holes in the 6T single crystal, at least in the absence of impurities and/or structural defects. These theoretical results do not agree with mobility measurements on 6T thin films and crystals, that reveal a predominant hole transport; this, however, is most likely the result of extrinsic effects related in particular to oxygen contamination [39].

It is interesting that the results collected in Fig. 3 for 6T clusters show a linear relationship between the bandwidths and $\cos(\pi/N+1)$, as would be expected in the framework of tight-binding models including only nearest-neighbor interactions [40]; thus, the valence and conduction bandwidths of infinite one-dimensional clusters can be extrapolated as four times the interchain transfer integral for holes and electrons, respectively. When considering all directions of transport, the *total* valence and conduction bandwidths built from the HOMO and LUMO levels are the key parameters for the description of band-like motion within the herringbone layers of the 6T crystals. The total valence bandwidth can be evaluated within a tight-binding model as the energy difference between, on the one hand, the most stable ''HOMO'' level of the crystal (characterized by a full bonding interchain overlap between the HOMO's of the interacting units) and, on the other hand, the less stable occupied level of the crystal (presenting the highest degree of antibonding interchain overlap). We then calculate a total width of 240 meV for the valence band in the LT phase, to be compared with a 50–15 meV value deduced from mobility measurements [20,21,41]. The INDO value for the total valence bandwidth in the HT phase of the 6T crystal is 328 meV; this is larger than that in the LT phase, in agreement with mobility measurements providing an estimate of

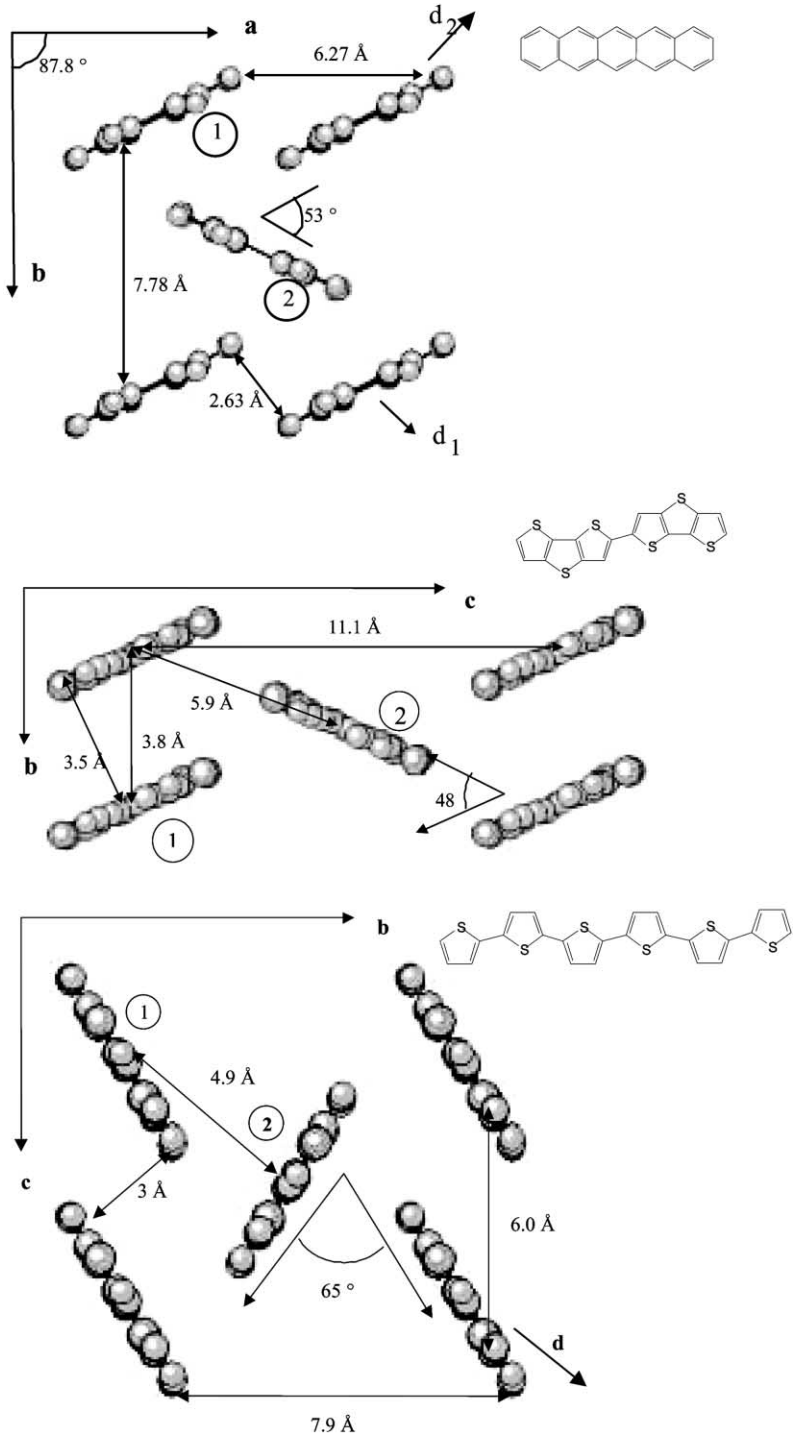

Fig. 2. Chemical structure and lattice parameters in the layers of: (top) crystalline pentacene; (middle) BDT; and (bottom) 6T. Labels 1 and 2 refer to the two inequivalent molecules in the unit cell.

470 meV [20,21]. Extended Hückel band-structure calculations give a value of 420 meV for the HT phase [42].

In the case of the pentacene single crystal, we calculate very large values of 608 and 588 meV for the total valence and conduction bandwidths, respectively. These theoretical results are fully consistent with recent experimental data, derived from mobility measurements on high-quality single crystals of pentacene, indicating bandwidths on the order of 500 meV both for electrons and holes [19]; the INDO results considerably improve the estimates provided by earlier Extended Hückel calculations [19].

The charge transport properties are markedly different in the BDT single crystal since the molecules are packed along the *b*-axis in nearly cofacial configurations. Significant

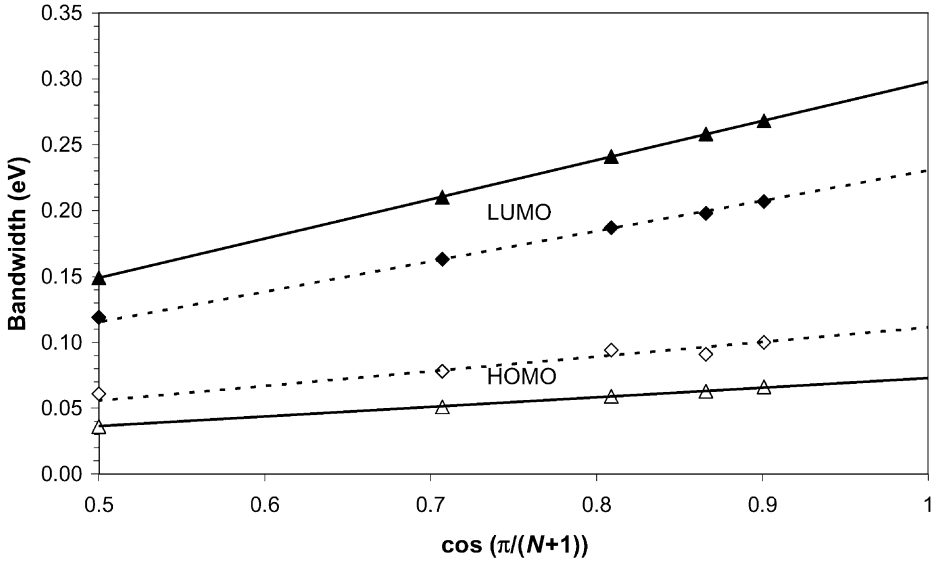

Fig. 3. Evolution of the INDO bandwidths formed by the HOMO (open symbols) and LUMO (filled symbols) levels of 6T molecules stacked along the *c*-axis (solid lines) and the diagonal axis *d* (dashed lines), as a function of $\cos(\pi/N+1)$, with N the number of molecules in the clusters.

electronic splittings are calculated only along the *b*-axis and there occur much larger interchain transfer integrals between the HOMO levels than between the LUMO levels (86 versus 14 meV). The theoretical splittings follow the cosine relationship versus *N*, yielding by extrapolation valence and conduction bandwidths of 344 and 56 meV, respectively. Charge transport in the BDT single crystal has, thus, a one-dimensional character with holes much more mobile than electrons.

All together, the theoretical results show that at low temperature, i.e. when the total bandwidth is the key parameter, the hole mobility is expected to be much higher in the pentacene single crystal than in 6T and BDT since the total valence bandwidth estimated for the latter two materials is much smaller than in pentacene. However, at room temperature, i.e. when the individual interchain transfer integrals between adjacent units come into play in the description of the hopping processes, the highest hole mobilities should be reached in the BDT single crystal, since BDT displays the largest interchain transfer integral for holes. This appears to be consistent with recent experimental data indicating that the room-temperature hole mobility in BDT thin films is much higher than in 4T and 6T thin films [43,44]. The results of our calculations also point out that the achievement of high charge mobilities along the organic semiconductor channel in field-effect transistors, requires a proper orientation of the layers within the crystals or thin films with respect to the surface on top of which they are deposited.

2.2. Highly organized polymer thin films

In the case of organized films of polymer chains, such as highly regioregular poly-3-hexylthiophene chains deposited by spin-coating on SiO_2/Si substrates in the form of highly organized lamellae lying perpendicular to the surface, recent experimental data show that the main direction for charge transport is perpendicular to the plane of the polymer backbones (even though a significant contribution is also observed along the chain axes) [45]. In similar experimental conditions, a lower degree of regioregularity along the polythiophene chains leads to a lamellar organization where the chains are lying flat on top of the surface, resulting in much lower charge mobilities along the channel.

Interestingly, it has been conjectured that the large hole mobilities measured for the highly regioregular poly-3-hexylthiophene RR-P3HT (on the order of 0.1 cm^2/V s at room temperature) reflect a delocalization of the charged species over several chains, which occurs because of both the small relaxation energy of polarons in large conjugated systems and the strong interaction between adjacent chains. The nature of the charge carriers in RR-P3HT has been investigated experimentally using optical charge modulation spectroscopy (CMS) [45] and photoinduced absorption (PiA) [46]. These studies have pinpointed substantial differences between the optical signatures of polarons in the microcrystalline materials, as compared to chemically doped polythiophene in solution. Such differences were attributed to delocalization of the polaronic species over several adjacent polythiophene chains, which is consistent with the high transport properties within the two-dimensional conjugated sheets [47,48].

The influence of interchain interactions on the optical absorption spectrum has been investigated by Blackman and Sabra in the case of doped polyacetylene [49] at the one-electron SSH (Su–Schrieffer–Heeger) level [50]. These authors have demonstrated that, for strong interchain coupling, charge delocalization occurs and is accompanied by a

dramatic change in the energies and relative intensities of the spectral transitions within the bandgap. Earlier local density functional theory (DFT) calculations by Vogl and Campbell on the crystal structure of polyacetylene suggested, on the basis of the magnitude of the interchain transfer integrals, that charges injected in perfect crystals would fully delocalize over a large number of conjugated chains and that, therefore, polarons would not be stable [51,52]. Similar DFT band-structure calculations on PPV have lead to the same conclusions [53]. An electron or hole injected in perfectly crystalline polyacetylene or PPV would then behave as a free charge carrier, without any lattice distortion. It was argued that the experimental observation of polarons in conjugated polymers reflects disorder in the films, which localizes the charge species [51–53].

Our theoretical approach here has first involved the computation of the geometric and electronic structures of a single five-ring oligophenylenevinylene chain (hereafter denoted PPV5) carrying a positive charge. Fig. 4 shows the bond-length deformations associated with the formation of a positive polaron on PPV5. Charge injection induces the appearance of a slight quinoid character on the phenylene rings, together with a decrease of bond-length alternation in the vinylene linkages. These deformations are more pronounced around the center of the molecule and typically extend over three repeat units (∼20 Å).

On the basis of the optimized geometry of the charged species, the one-electron energy levels were calculated at the INDO level. A simplified representation of the one-electron diagrams is given in Fig. 5. Removal of one electron from a conjugated chain induces the appearance of two electronic (polaronic) levels within the previously forbidden HOMO–LUMO gap [9]. The localized character of these gap levels is easily confirmed from the evaluation of the electronic density computed at the INDO level for the PPV5 molecule.

The computation of the excited states has been performed at two different levels: (i) the Austin model 1/configuration interaction (AM1/CI) formalism; and (ii) an INDO/SDCI method where all single excitations over the electronic-p levels and a limited number of double excitations (over 16 MOs) are involved. As seen from Fig. 6, most of the optical absorption cross-section of the charged species is shared between two excited states mainly described in terms of the C1 and C2 electronic transitions of Fig. 5. Denoting HOMO as the highest doubly occupied level, P1 as the lowest (singly occupied) polaronic level, and P2 as the highest (empty) polaronic level, C1 and C2 correspond to single HOMO → P1 and P1 → P2 excitations, respectively [54].

The presence of two dominant absorption bands is in good agreement with experimental data on monoionic oligo(phenylenevinylene) solutions [55]. For the five-ring oligomer studied here, two main optical transitions are measured around 0.72 and 1.63 eV, which compare well with both the AM1/CI (0.82 and 1.92 eV) and INDO/SDCI (0.96 and 1.81 eV) results. The chain-length evolution of the positions and relative intensities of these electronic transitions is also well reproduced by both formalisms [56].

The influence of interchain interactions on the optical response of singly charged polarons has been assessed by considering a cofacial aggregate formed by two five-ring PPV chains separated by 4 Å. This configuration is similar to that encountered in the microcrystalline domains of RR P3HT [45]. For such a symmetric cofacial arrangement, the INDO and AM1 approaches lead to molecular orbitals completely delocalized over the two conjugated chains.

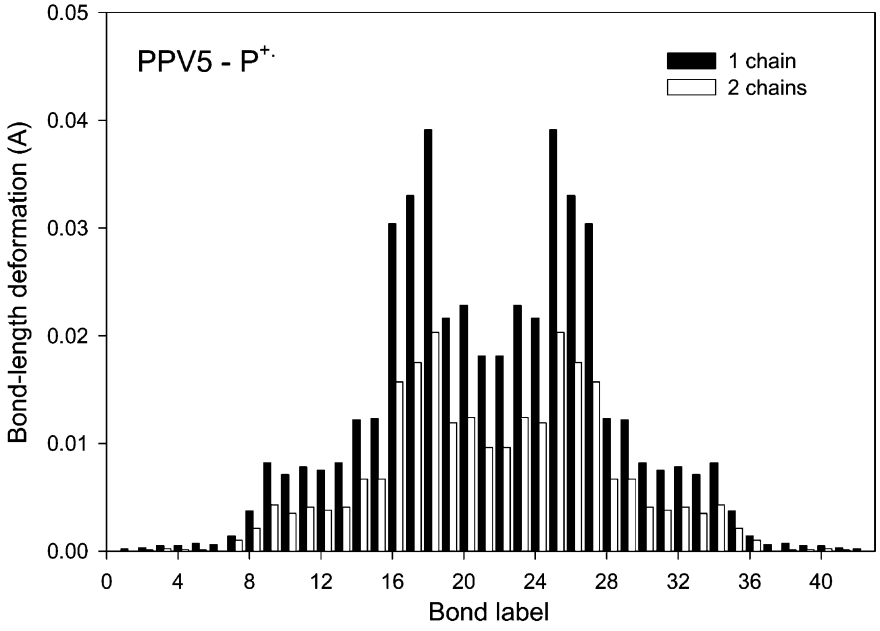

Fig. 4. Differences (in Å) between the AM1/CI calculated bond lengths in the neutral and singly charged states of PPV5, in the isolated molecule (black) and in the dimer (gray).

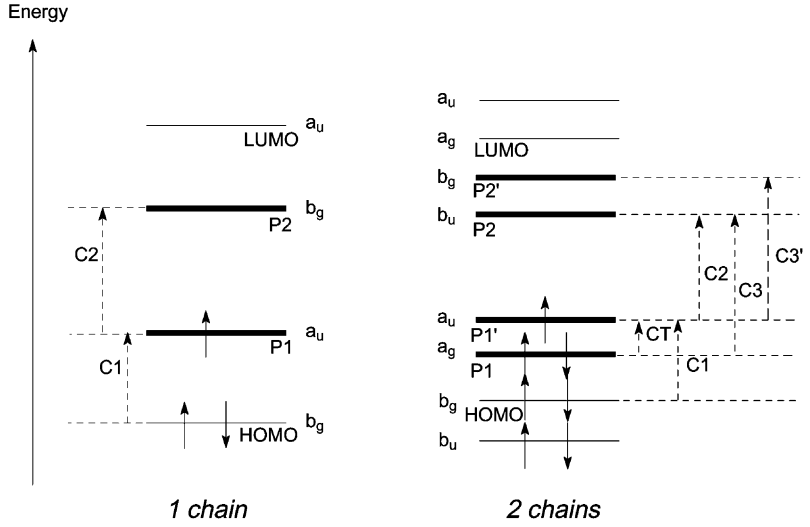

Fig. 5. Schematical representation of the one-electron energy diagram for a polaron: (i) localized on a single conjugated chain (left); and (ii) delocalized over two cofacial chains (right). The symmetry of the orbitals and the relevant electronic excitations are indicated.

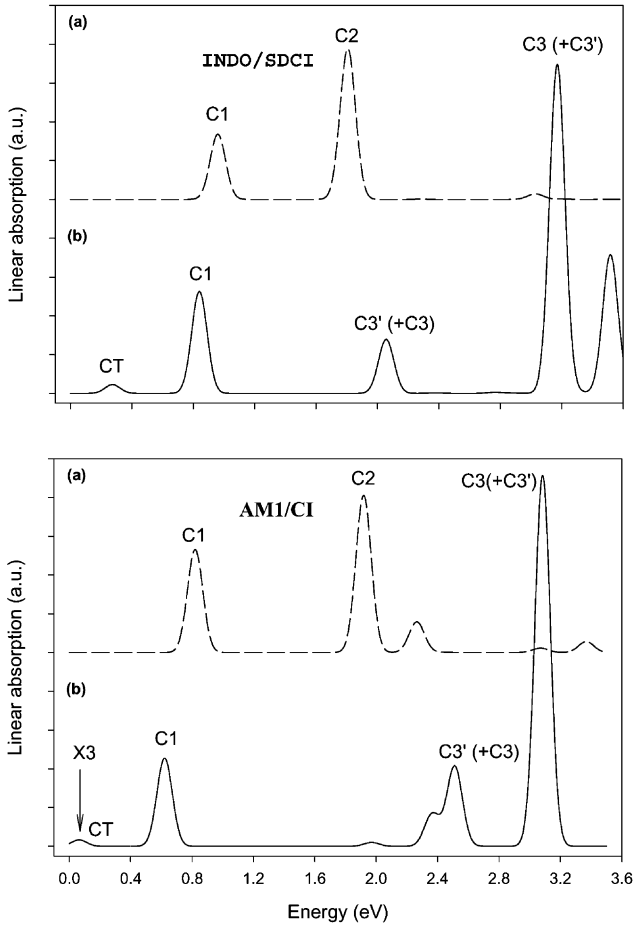

Fig. 6. Top: linear absorption spectra of: (a) the singly charged PPV5 single molecule; and (b) the cofacial dimer, simulated on the basis of the INDO/SDCI description of the excited states. Bottom: similar results from AM1/CI calculations. Gaussian functions with 0.05 eV width at half maximum have been used to convolute the spectra.

The lattice deformations in the aggregate are compared to those calculated for the isolated molecule in Fig. 4. Since the perturbation induced by charge injection in the individual chains of the dimer is weaker than in the single-chain case, the bond-length modifications are less pronounced in the aggregate (especially around the center of the molecule) and extend in a symmetric way over the two conjugated chains.

In a cofacial dimer with C_{2h} symmetry, interchain coupling leads to a splitting of all electronic levels into *gerade/ungerade* symmetry molecular orbital pairs, see Fig. 5. The absorption spectrum of the cationic dimer can then be interpreted on the basis of a one-electron energy diagram, wherein *four* polaronic levels (one doubly occupied, one singly occupied, and two empty) are pushed within the HOMO–LUMO gap as a result of wavefunction localization (these orbitals are referred to as P1, P1′, P2, and P2′) [56]. Note that the four polaronic levels extend in a symmetric way over the two chains. In contrast, in the SSH calculations of Blackman and Sabra, only two electronic levels are found inside the bandgap, whatever the strength of interchain interactions [49].

The absorption spectrum of the cationic dimer is shown in comparison to that of the one-chain polaron in Fig. 6. [56] The weaker lattice relaxation in the two-chain aggregate translates into shallower drifts of the polaronic levels inside the gap and a consequent red-shift (by 0.1–0.2 eV) of the absorption band described by the C1 electronic excitation. The nature of the latter transition remains essentially unaffected by interchain interactions.

The most striking feature in the optical spectrum of the singly charged dimer is the appearance of a *new intense optical transition* located around 3.1 [3.2] eV at the AM1/CI [INDO/SDCI] level and the emergence of a weak signal, denoted CT, around 0.1 [0.25] eV. Single particle excitations

between the four polaronic electronic levels produce *two* excited states with B_u symmetry (i.e. one-photon symmetry allowed with respect to the ground state), instead of one in the single-chain limit (note that C2 is symmetry forbidden in the dimer). These two B_u excited states result from the configuration mixing between the C3 and C3′ electronic transitions. Constructive combination of these optical excitations leads to the spectral feature around 3.1 eV (i.e. just below the optical gap of the neutral system (∼3.2 eV)), which dominates the absorption spectrum of the two-chain aggregate, see Fig. 6. Destructive coupling between the same configurations provides the weaker absorption line around 2.4 [2.1] eV (note that this excited state also involves significant contributions from doubly excited configurations).

The charge-transfer CT optical transition in Fig. 6 is polarized along the interchain packing axis, while all other absorption bands are mainly polarized along the chain axis. The intensity of this absorption feature is controlled by the amount of delocalization in the polaron wavefunction; the overlap between the electron and hole wavefunctions of the CT pair and therefore also the transition moment is maximum for full delocalization over the two conjugated segments, while it is vanishingly small for polarons that would be constrained on isolated chains [57]. In addition, the absorption cross-section also depends linearly on the excitation energy of the CT transition, that is to say the energy separation between the two occupied polaronic levels P1 and P1′, which also peaks in the limiting case of complete delocalization. Thus, the optical cross-section of this absorption band gives a direct information on the effectiveness of interchain charge delocalization in the conjugated materials. The theoretical simulations presented here are fully consistent with the changes in optical absorption observed experimentally when improving the degree of interchain order in alkyl-substituted polythiophene derivatives [45,46,56].

A similar description is expected to hold in the case of a larger number of cofacial interacting molecules as well as for aggregates with lower symmetry (as long as the interchain interactions are strong enough to delocalize the excess charge) [57]. Delocalization of the polaron over *N* conjugated chains would result in the formation of a pair of *N*-level polaronic bands inside the gap, a nearly filled band (minus one electron for a positive polaron) and an empty one. Charge-carrier interchain mobilities in conjugated polymers can be related to the width of these bands (which is directly related to the strength of the interchain interactions) and the energy departure from the valence and conduction bands (quantified by the polaron relaxation energy), which can be both monitored by means of spectroscopic tools. Full delocalization of the charges over an infinite number of conjugated chains would lead to vanishingly small geometric relaxation phenomena and, hence, negligible relaxation energies; very high (band-like) charge-carrier mobilities can then be expected. The intermediate mobilities reported for the regioregular substituted poly-alkylthiophenes [56] suggest that, although the degree of order allows for some spreading of the polaron wavefunction over several chains, such a band type charge transport mechanism is not achieved yet.

Finally, we emphasize that polymers offer the advantage over small molecules of smaller polaron relaxation energies. As a result, the turn-over from polaron-like to band-like transport might occur at a lower degree of interchain order.

Acknowledgements

We wish to warmly thank Alan Heeger, Alan MacDiarmid, and Hideki Shirakawa for their pioneering role and major contributions to the field of Synthetic Metals. The constant inspiration they provided us over the past twenty years has greatly impacted our work. We are also very much indebted to both Alans for the stimulating collaborations which we had the privilege to conduct with them. The work at Arizona is partly supported by the National Science Foundation (CHEM-0078819), the Office of Naval Research, and the Petroleum Research Fund. The work in Mons is partly supported by the Belgian Federal Government ''Interuniversity Attraction Pole in Supramolecular Chemistry and Catalysis (PAI 4/11)'' and the Belgian National Fund for Scientific Research (FNRS/FRFC). The work at MIT is partly supported by NSF. D. Beljonne and J. Cornil are Research Associates of FNRS.

References

[1] B.E. Kohler, Chem. Rev. 93 (1993) 41.
[2] L. Salem, Molecular Orbital Theory of Conjugated Systems, Benjamin, New York, 1966.
[3] A. Szabo, N.S. Ostlund, Modern Quantum Chemistry, Macmillan, New York, 1982.
[4] M. Pope, C. Swenberg, Electronic Processes in Organic Materials, Oxford University Press, New York, 1982
[5] M. Pope, C.E. Swenberg, Electronic Processes in Organic Crystals and Polymers, Oxford University Press, New York, 1999.
[6] Z.G. Soos, D.S. Galvao, S. Etemad, Adv. Mater. 6 (1994) 280.
[7] W.P. Su, J.R. Schrieffer, A.J. Heeger, Phys. Rev. Lett. 42 (1979) 1698.
[8] A.J. Heeger, S. Kivelson, J.R. Schrieffer, W.P. Su, Rev. Mod. Phys. 60 (1988) 781.
[9] J.L. Brédas, G.B. Street, Acc. Chem. Res. 18 (1985) 309.
[10] J. Cornil, D. Beljonne, J.L. Brédas, Synth. Met. 85 (1997) 1029.
[11] Z.G. Soos, S. Ramasesha, D.S. Galvao, Phys. Rev. Lett. 71 (1993) 1609.
[12] J.H. Burroughes, D.D.C. Bradley, A.R. Brown, R.N. Marks, K. Mackay, R.H. Friend, P.L. Burn, A.B. Holmes, Nature 347 (1990) 539.
[13] G. Gustaffson, Y. Cao, G.M. Treacy, F. Klavetter, N. Colaneri, A.J. Heeger, Nature 357 (1992) 477.
[14] V.M. Kenkre, J.D. Anderson, D.H. Dunlap, C.B. Duke, Phys. Rev. Lett. 62 (1989) 1165.
[15] H. Bässler, Phys. Stat. Sol. (b) 175 (1993) 15.
[16] M.W. Wu, E.M. Conwell, Chem. Phys. Lett. 266 (1997) 363.
[17] P.M. Borsenberger, D.S. Weiss, Organic Photoreceptors for Xerography, Marcel Dekker, New York, 1998.

[18] M.A. Palenberg, R.J. Silbey, M. Malagoli, J.L. Brédas, J. Chem. Phys. 112 (2000) 1541.
[19] J.H. Schön, C. Kloc, B. Batlogg, Science 288 (2000) 2338.
[20] J.H. Schön, C. Kloc, B. Batlogg, Synth. Met. 115 (2000) 75.
[21] J.H. Schön, S. Berg, C. Kloc, B. Batlogg, Mat. Res. Soc. Symp. Proc. 588 (2000) BB 9.5.
[22] J.K. Burdett, Chemical Bonding in Solids, Oxford University Press, New York, 1995.
[23] R.A. Marcus, Rev. Mod. Phys. 65 (1993) 599.
[24] P.F. Barbara, T.J. Meyer, M.A. Ratner, J. Phys. Chem. 100 (1996) 13148.
[25] V. Balzani, A. Juris, S. Campagna, S. Serroni, Chem. Rev. 96 (1996) 759.
[26] K. Sakanoue, M. Motoda, M. Sugimoto, S. Sakaki, J. Phys. Chem. A 103 (1999) 551.
[27] M. Malagoli, J.L. Brédas, Chem. Phys. Lett. 327 (2000) 13.
[28] J.H. Schön, S. Berg, C. Kloc, B. Batlogg, Science 287 (2000) 1022.
[29] J.H. Schön, C. Kloc, B. Batlogg, Phys. Rev. Lett. 86 (2001) 3843.
[30] A. Devos, M. Lannoo, Phys. Rev. B 58 (1998) 8236.
[31] J. Ridley, M.C. Zerner, Theoret. Chim. Acta 32 (1973) 111.
[32] M.C. Zerner, G.H. Loew, R.F. Kichner, U.T. Mueller-Westerhoff, J. Am. Chem. Soc. 102 (1980) 589.
[33] N. Mataga, K. Nishimoto, Z. Phys. Chem. 13 (1957) 140.
[34] M.D. Newton, Int. J. Quant. Chem. 77 (2000) 255.
[35] G. Horowitz, B. Bachet, A. Yassar, P. Lang, F. Demanze, J.L. Fave, F. Garnier, Chem. Mater. 7 (1995) 1337.
[36] T. Siegrist, R.M. Fleming, R.C. Haddon, R.A. Laudise, A.J. Lovinger, H.E. Katz, P. Bridenbaugh, D.D. Davis, J. Mater. Res. 10 (1995) 2170.
[37] X.C. Li, H. Sirringhaus, F. Garnier, A.B. Holmes, S.C. Moratti, N. Feeder, W. Clegg, S.J. Teat, R.H. Friend, J. Am. Chem. Soc. 120 (1998) 2206.
[38] J. Cornil, J.Ph. Calbert, J.L. Brédas, J. Am. Chem. Soc. 123 (2001) 1250.
[39] G. Horowitz, Adv. Mater. 10 (1998) 365.
[40] J. Cornil, J.Ph. Calbert, D. Beljonne, D.A. dos Santos, J.L. Brédas, Mat. Res. Soc. Symp. Proc. 588 (2000) BB1.4/1–7.
[41] L. Torsi, A. Dodabalapur, L.J. Rothberg, A.W.P. Fung, H.E. Katz, Phys. Rev. B 57 (1998) 2271.
[42] R.C. Haddon, T. Siegrist, R.M. Fleming, P.M. Bridenbaugh, R.A. Laudise, J. Mater. Chem. 5 (1995) 1719.
[43] H. Sirringhaus, R.H. Friend, X.C. Li, S.C. Moratti, A.B. Holmes, N. Feeder, Appl. Phys. Lett. 71 (1997) 3871.
[44] F. Garnier, private communication.
[45] H. Sirringhaus, P.J. Brown, R.H. Friend, M.N. Nielsen, K. Bechgaard, B.M.W. Langeveld-Voss, A.J.H. Spiering, R.A.J. Janssen, E.W. Meijer, P. Herwig, D.M. de Leeuw, Nature 401 (1999) 685.
[46] R. Österbacka, C.P. An, X.M. Jiang, Z.V. Vardeny, Science 287 (2000) 839.
[47] Z. Bao, A. Dodabalapur, A. Lovinger, Appl. Phys. Lett. 69 (1998) 4108.
[48] H. Sirringhaus, N. Tessler, R.H. Friend, Science 280 (1998) 1741.
[49] J.A. Blackman, M.K. Sabra, Phys. Rev. B 47 (1993) 15437.
[50] W.P. Su, J.R. Schrieffer, A.J. Heeger, Phys. Rev. B 22 (1980) 2099.
[51] P. Vogl, D.K. Campbell, Phys. Rev. Lett. 62 (1989) 2012.
[52] P. Vogl, D.K. Campbell, Phys. Rev. B 41 (1990) 12797.
[53] P. Gomes da Costa, R.G. Dandrea, E.M. Conwell, Phys. Rev. B 47 (1993) 1800.
[54] J. Cornil, J.L. Brédas, Adv. Mater. 7 (1995) 295.
[55] R. Schenk, H. Gregorius, K. Müllen, Adv. Mater. 3 (1991) 492.
[56] D. Beljonne, J. Cornil, H. Sirringhaus, P.J. Brown, M. Shkunov, R.H. Friend, J.L. Brédas, Adv. Funct. Mat. 11 (2001) 229.
[57] D. Beljonne, et al., submitted for publication.